J Electr Eng Technol Vol. 9, No. 3: 1080-1088, 2014
http://dx.doi.org/10.5370/JEET.2014.9.3.1080

ISSN(Print) 1975-0102
ISSN(Online) 2093-7423

Optimization of Wind Power Dispatch to Minimize Energy Storage System Capacity

Cong-Long Nguyen* and Hong-Hee Lee†

Abstract – By combining a wind turbine with an energy storage system (ESS), we are able to attenuate the intermittent wind power characteristic making the power derived from a wind farm dispatchable. This paper evaluates the influence of the phase delay of the low-pass filter in the conventional smoothing power control on the ESS capacity; longer phase delays require a larger ESS capacity. In order to eliminate the effect of the phase delay, we optimize the power dispatch using a zero-phase low-pass filter that results in a non-delayed response in the power dispatch. The proposed power dispatching method significantly minimizes the ESS capacity. In addition, the zero-phase low-pass filter, which is a symmetrical forward-reverse finite impulse response type, is designed simply with a small number of coefficients. Therefore, the proposed dispatching method is not only optimal, but can also be feasibly applied to real wind farms. The efficacy of the proposed dispatching method is verified by integrating a 3 MW wind turbine into the grid using wind data measured on Jeju Island.

Keywords: Wind energy conversion systems (WECS), Energy storage system (ESS), Wind power dispatching methods, Zero-phase low-pass filter

1. Introduction

In order to solve the global issues surrounding the dwindling fossil fuel resources and climate change, efforts to harness renewable energy sources such as wind, solar, and tidal power have attracted a great deal of attention [1]. Among these renewable sources, wind energy has developed rapidly and has become the most promising candidate for power supply to electrical grid systems in the near future [2, 3]. However, wind power generation is unsteady and uncontrollable because wind speed inherently depends on natural meteorological conditions. Moreover, the introduction of large amounts of intermittent power to the grid can bring about serious technical challenges such as grid interconnection, power quality, and system reliability [4, 5]. Therefore, wind farm (WF) developers need to overcome the intermittent nature of wind power before attempting to dispatch high levels of power to the grid.

In order to mitigate the fluctuation in wind power, the pitch angle control for a variable-speed wind turbine generator is introduced. The pitch angle is controlled to regulate the wind turbine (WT) output power following a smoothened power reference; however, this method increases system complexity, and the WT might not capture the maximum power of the wind [6]. Recently, the utilization of energy storage systems (ESSs) as an energy buffer to compensate for wind power fluctuation has been proposed and investigated in several literatures [7-17]. Compared with previous solutions, ESSs can help wind energy conversion systems harness the maximum available wind power; this valuable outcome is actually the most fundamental demand in renewable energy systems.

Thanks to the rapid development of energy storage devices such as batteries, super-conducting magnetic energy storage (SMES), electric double-layer capacitors (EDLC), and flywheels, these storage systems could feasibly handle the intermittent characteristic of wind power [12]. However, a large-scale ESS is still rather expensive; therefore, the use of a minimal-capacity ESS is a critical necessity to reduce overall system cost.

Integration of ESS to WF results in a hybrid system in which the harnessed wind power is separated into two power components: stable power, which is delivered to the grid, and fluctuating power, which is released or stored by the ESS [13]. Therefore, the power of ESS depends completely on the power dispatch. In other words, to minimize ESS capacity for a WF, wind power dispatched to the grid needs to be well-defined. In [8-10], the power dispatch is planned by taking the average wind power ahead of time for every dispatching time interval. Meanwhile, in [11] and [12], the power dispatch is determined using the maximum or minimum levels of wind power in each dispatching interval, which depends on whether the ESS is charging or discharging. Both of these dispatching strategies require an advance wind power forecast of several hours, and they involve a complicated process to manage power dispatch in the short-term. Another dispatching method is an application of the low-pass filter, where the power dispatch is determined

† Corresponding Author: School of Electrical Engineering, University of Ulsan, Korea. (hhlee@mail.ulsan.ac.kr)
* School of Electrical Engineering, University of Ulsan, Korea. (conglongbk@gmail.com)
Received: November 19, 2013; Accepted: March 7, 2014

by smoothing the wind power through a low-pass filter [13-17]. This dispatching method is easy to implement and results in a small ESS power fluctuation, making it more feasible for controlling the power dispatch when compared with the aforementioned dispatching methods. However, because the filters used in this dispatching method are a first-order or a second-order infinite impulse response (IIR) low-pass type, the phase delay is essentially inevitable in the pass-band region. This causes a lag in the response of the dispatched power, which leads to an increase in ESS capacity.

In this paper, we eliminate the phase delay in the smoothing dispatch method in order to optimize the power dispatch, thereby minimizing ESS capacity. The proposed dispatching method utilizes a zero-phase low-pass filter (ZPLPF) that is a symmetrical forward-reverse finite impulse response (FIR) type. Although this idea was introduced succinctly in [14], some weak points in the design and implementation of the dispatching method remain. To overcome these problems, the ZPLPF is designed simply with a small number of coefficients. In addition, we introduce a method to determine a suitable smoothing time constant for the dispatching method.

The paper is organized as follows. Section 2 presents the configuration of the ESS connected to the WF and defines the required ESS capacity. In Section 3, an optimal dispatching power control via the application of a FIR ZPLPF is proposed in order to overcome the disadvantage of the conventional smoothing dispatch method that is based on the IIR type. In Section 4, we introduce the process of how to determine a suitable smoothing time constant for the proposed dispatching method. Next, in Section 5, several numerical examples with a 3 MW WT model are studied using real wind speed data measured on Jeju Island in order to demonstrate the effectiveness of the proposed dispatching method. Finally, the paper is concluded in Section 6.

2. Energy Storage Systems in Wind Farms

Fig. 1 shows the typical output power profile of a WT over the course of one week. Wind power might increase rapidly to reach $1\ p.u.$ or drop suddenly to zero, indicating

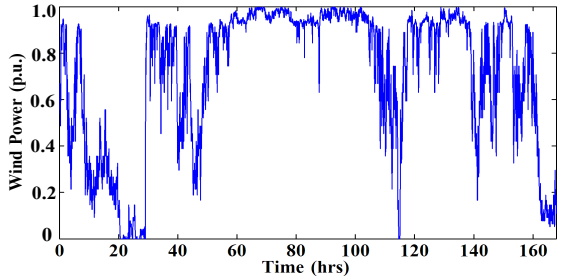

Fig. 1. The typical output power of a WT over the course of one week.

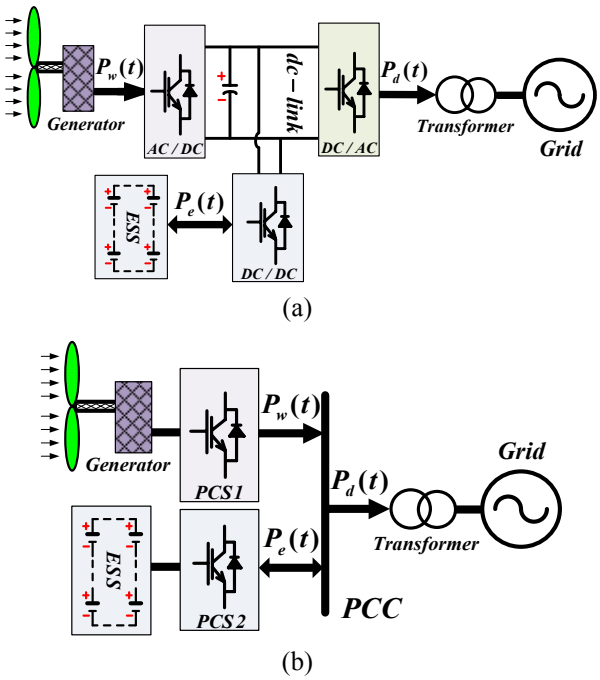

Fig. 2. Configurations of the ESS-wind hybrid power system: (a) The ESS connected to the dc-link; (b) The ESS connected directly to the grid.

that wind is a non-dispatchable energy resource. In order to solve this intermittent characteristic of the wind resource, the ESS is aggregated with the WT.

2.1 Wind turbines with energy storage systems

Integration of the ESS into a WF results in a wind-ESS hybrid power system; the configurations of this system are illustrated in Fig. 2. In Fig. 2(a), a back-to-back converter is adopted to provide grid connection capabilities. The output of the generator, $P_w(t)$, is rectified and stored in the dc-link where the ESS is also connected via a bidirectional DC-to-DC converter. This bidirectional converter is capable of delivering a negative or positive power, $P_e(t)$, enabling it to discharge or charge the ESS. In Fig. 2(b), the ESS and the WT generator are independently connected to the grid at the point of common coupling (PCC) through the power conversion systems *PCS1* and *PCS2*, respectively. Among the many kinds of WT generators used in industrial WFs, the permanent magnet synchronous generator (PMSG) and the doubly fed induction generator (DFIG) are the most popular [18]. To integrate the ESS into the PMSG-based system, the configuration shown in Fig. 2(a) is usually employed. Meanwhile, the configuration in Fig. 2(b) is recommended for the hybrid ESS and DFIG-based WT systems.

2.2 Definition of the required ESS capacity

If we neglect the power losses in the system, the ESS power, $P_e(t)$, can be calculated by:

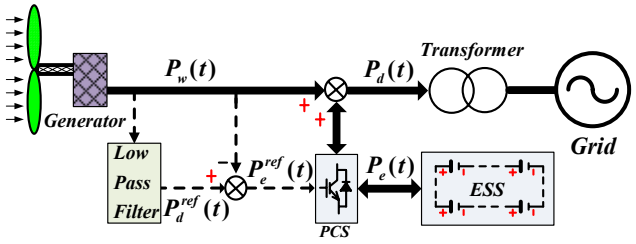

Fig. 3. Smoothing power control of the wind-ESS hybrid system.

$$P_e(t) = P_d(t) - P_w(t) . \quad (1)$$

From (1), the ESS power depends not only on the wind power captured by the WT, $P_w(t)$, but also on the power dispatch, $P_d(t)$.

Fig. 3 illustrates the whole control scheme of a wind-ESS hybrid power system utilizing a low-pass filter to decide power dispatch. By smoothing the WT output power through the filter, the power dispatch reference, $P_d^{ref}(t)$, is obtained. The difference between the reference and the WT output power is the ESS desired power, $P_e^{ref}(t)$:

$$P_e^{ref}(t) = P_d^{ref}(t) - P_w(t) . \quad (2)$$

The power conversion system (PCS) controls whether the ESS is charging or discharging according to the reference, $P_e^{ref}(t)$. If the PCS satisfies its reference, i.e., $P_e(t) = P_e^{ref}(t)$, then the power dispatch also success-fully tracks its reference as proven by the following:

$$P_d(t) = P_w(t) + P_e(t) = P_w(t) + [P_d^{ref}(t) - P_w(t)] = P_d^{ref}(t) . \quad (3)$$

In Fig. 4, the system performance including the WT output power and power dispatch is shown in order to demonstrate that the fluctuation in wind power can be suppressed to supply stable power for the grid.

The required ESS capacity, which is normally specified in terms of energy rating, E_e^{rat}, and power rating, P_e^{rat}, can be defined based on the WT output power and power dispatch [8], 16]. The ESS power rating is defined in (4) during the system operating time interval, T:

$$P_e^{rat} = \underset{0 \le t \le T}{MAX} | P_e(t) | = \underset{0 \le t \le T}{MAX} | P_d(t) - P_w(t) | . \quad (4)$$

In Fig. 4(b), the ESS power is plotted as a function of the WT output power and the power dispatch profile given in Fig. 4(a). During the considered time interval T, the ESS power is greatest at instant t_1, which thereby defines the ESS power rating. By integrating the ESS power with respect to time, we can obtain the net energy, $E_e(t)$, supplied to or drawn from the storage up to time, t:

$$E_e(t) = \int_0^t P_e(\tau) d\tau = \int_0^t [P_d(\tau) - P_w(\tau)] d\tau . \quad (5)$$

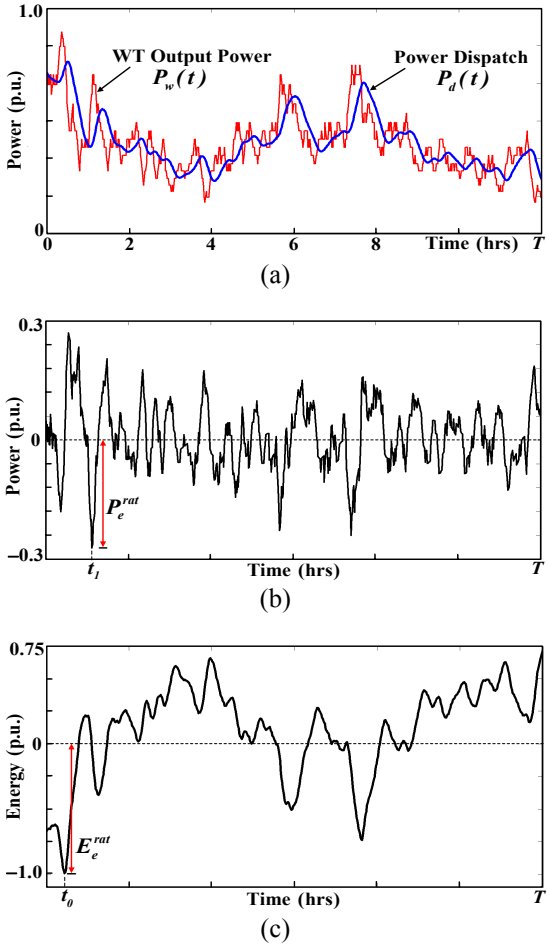

Fig. 4. ESS-wind hybrid system performance: (a) WT output power and power dispatched to the grid; (b) ESS power; (c) ESS energy with respect to time.

The ESS energy rating expresses the maximum capacity that can be stored or released. This is defined as follows:

$$E_e^{rat} = \underset{0 \le t \le T}{MAX} | E_e(t) | . \quad (6)$$

Fig. 4(c) illustrates the ESS energy profile, in which the energy capacity is designated at instant t_0, when the ESS stores the maximum energy.

3. Optimal Power Dispatch of Wind-ESS Hybrid Systems

The ESS capacity depends on how the system dispatches power into the grid; an optimal power dispatch results in the minimum required ESS capacity. In smoothing power control, because the power dispatch is determined through the low-pass filter, optimization of power dispatch means optimizing the filter. First, we investigate the current drawbacks of the conventional smoothing method that is based on an IIR-type low-pass filter (IFLPF).

3.1 Phase delay problems in the conventional dispatching method

An IFLPF is usually adopted in a conventional smoothing power dispatch method [13], which is described mathematically as:

$$G(s) = \frac{1}{1 + sT_c}, \tag{7}$$

where T_c is a smoothing time constant. With a longer T_c, the dispatched power has less fluctuation, as shown in Fig. 5(a). The power dispatches for the smoothing time constants $T_c = 20T_s$ and $T_c = 100T_s$, where T_s is the system sampling time, are plotted together with wind power. Even though the dispatching power control is robust and easy to implement, the response delay is inevitable. The delay problem clearly appears at instant t_1 or t_3 when the dispatched power is delayed for a period of time $\Delta t = t_2 - t_1$ from the wind power. In addition, the time delay increases with a larger smoothing time constant, which induces a much higher ESS power. In Fig. 5(b), the ESS power in these two cases is plotted to demonstrate the effect of the delay.

The time delay in the dispatch power is caused by the inevitable phase delay of the low-pass filter whose Bode diagram is plotted in Fig. 6. Within the filter pass-band area, the filter has a phase lag which causes the delayed response. Therefore, it is clear that the conventional dispatching method based on the low-pass filter does not yield an optimal power dispatch, but causes an increase in the required ESS capacity.

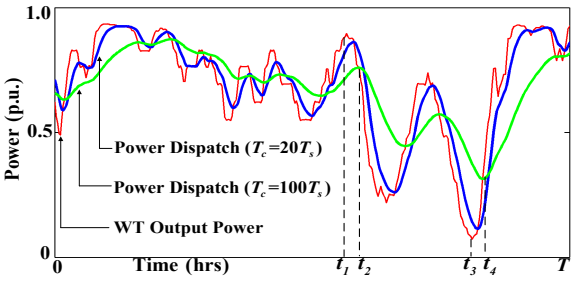

(a)

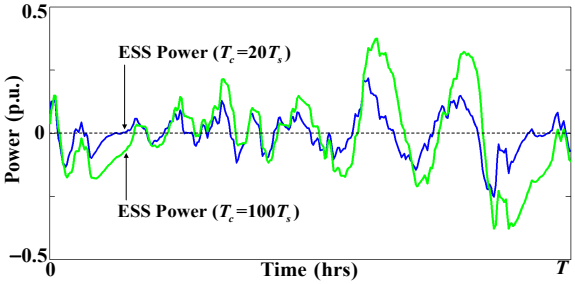

(b)

Fig. 5. System performance of the conventional dispatching method in two different smoothing time constants: (a) Power dispatch and wind power and (b) ESS power.

3.2 Proposed dispatching method with a zero-phase low-pass filter

In order to eliminate the response delay due to the phase lag of the low-pass filter in the conventional smoothing power dispatching method, we propose an effective dispatching strategy based on a ZPLPF. Although the basic idea of eliminating the phase delay to minimize ESS capacity has been presented in [14], their method requires a high-order FIR filter (over 50 orders) and the process involved in determining the filter coefficients is complicated, which makes this method difficult to implement in practice. Fig. 7 shows a filter with the desirable low-pass filter characteristics of the proposed power dispatching method. This type of filter is referred to as a ZPLPF [21]. In the pass-band region ($\omega \le \omega_c$), the phase and the magnitude should be zero degrees and decibels (dB), respectively. Meanwhile, in the stop-band region ($\omega > \omega_c$), the magnitudes should be as small as possible. To design a filter with a reduced number of coefficients, a symmetrical forward-reverse digital FIR filter is applied, which is defined as follows:

$$H(z) = \alpha_N z^N + \ldots + \alpha_1 z + \alpha_0 + \alpha_1 z^{-1} + \ldots + \alpha_N z^{-N}. \tag{8}$$

Its frequency response can be derived as

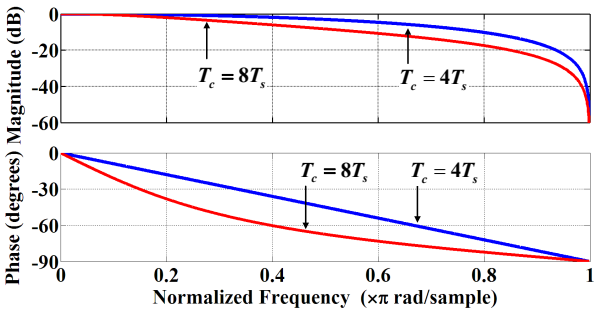

Fig. 6. Bode diagram of the filter with the conventional dispatching method.

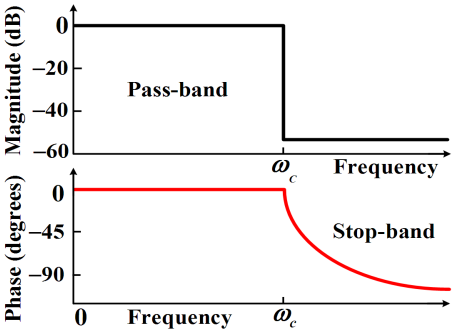

Fig. 7. Desirable bode diagram of the filter in the proposed dispatching power method.

$$H(e^{j\omega T_s}) = \alpha_N e^{jN\omega T_s} + \ldots + \alpha_1 e^{j\omega T_s} + \alpha_0 + \alpha_1 e^{-j\omega T_s} + \ldots + \alpha_N e^{-jN\omega T_s}$$
$$= \alpha_0 + 2\sum_{k=1}^{N} \alpha_k \cos(k\omega T_s) . \quad (9)$$

The frequency response is clearly real when all coefficients, α_k, are real, which leads to a zero-delay time response for the filter. In other words, the delay problem in the conventional dispatching method can be successfully overcome by adopting the proposed method.

Performance of the ZPLPF defined in (8) depends on the length (N) of its coefficient [22]. When N is reduced, the method becomes easier to implement, but the filter quality in the stop-band becomes worse. Therefore, we should assign a suitable N that achieves a reasonable trade-off between ease of implementation and quality. In this paper, the filter is designed to achieve a simple computation and 40 dB attenuation in the band-pass region; N is set to 5 and the filter coefficients are determined according to the impulse response of the first-order low-pass filter [23]. We define an array (h) containing first N values of the impulse response of the first-order low-pass filter as

$$h = \left[h_0 \ \ldots \ h_k \ \ldots \ h_N \right], \quad (10)$$

where

$$h_k = \frac{1}{T_c} e^{\frac{-k}{T_c}} ; \ \ k = 0, 1, \ldots, N . \quad (11)$$

Then, h is convolved with itself and normalized to yield the coefficients of ZPLPF as (12) and (13).

$$\tilde{\alpha}_k = \sum_{n=k}^{N} h_n h_{n-k} ; \ \ k = 0, 1, \ldots, N \quad (12)$$

$$\alpha_k = \frac{\tilde{\alpha}_k}{\tilde{\alpha}_0 + 2\sum_{n=1}^{N} \tilde{\alpha}_n} ; \ \ k = 0, 1, \ldots, N . \quad (13)$$

Fig. 8 shows the Bode diagram of the IFLPF in the conventional dispatching power method and the designed ZPLPF in the proposed method. We can see that the proposed method eliminates the phase delay problem and maintains the desired attenuation level when compared with the conventional smoothing method.

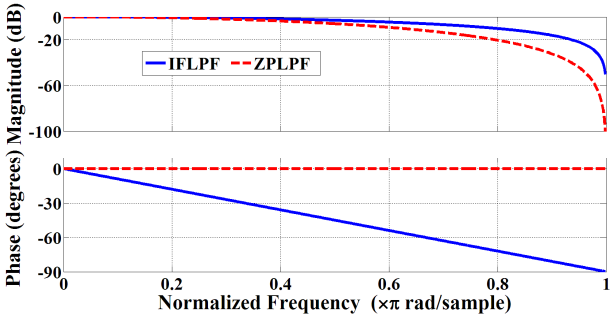

Fig. 8. Bode diagram of the IFLPF and the designed ZPLPF when the smoothing time constant is $T_c = 4T_s$.

The proposed dispatching method with the ZPLPF defined in (8) contains N forward components. Thus, the proposed method requires N wind power samples ahead of time to determine the power dispatch. During the planning and design stages of the wind-ESS hybrid system, this requirement is of little concern because the wind power profile is given. Meanwhile, to control the short-term power dispatch, we must forecast the wind power. However, because N is small ($N = 5$), N wind power samples can be forecasted accurately [20]. Therefore, the proposed dispatching power method is not only an optimal power dispatching solution, but has the potential to be easily implemented.

4. Determination of the Smoothing Time Constant

The proposed dispatching method in Fig. 3 determines the power dispatch based on the designed ZPLPF. In the system, the fluctuating suppression level of the wind power is decided by the smoothing time constant of the filter. The current challenge is to select a suitable T_c such that the dispatched power satisfies the fluctuation limit within a window of time [15]. In order to plan and control the system according to the dispatching method, T_c must be defined.

First, the fluctuation level of power dispatched in the i^{th} $\rho-\min$ window of time is defined as a percentage of the WT power rating P_{WTR}:

$$\Delta P^i_{\rho\min} = \frac{\underset{(i-1)\rho\le t<i\rho}{MAX}\{P_d(t)\} - \underset{(i-1)\rho\le t<i\rho}{MIN}\{P_d(t)\}}{P_{WTR}} 100\% \quad (14)$$

To dispatch wind power into the grid, the fluctuation level must be less than the limitation that is given by the electric power system where WF integrated into,

$$\Delta F_{\rho\min} = \underset{\forall i}{MAX}\left\{\Delta P^i_{\rho\min}\right\} \le \gamma_{\rho\min} \quad (15)$$

Usually, the power fluctuation levels in two time windows (1 min and 30 min) are considered. Hence, the smoothing time constant, T_c, must be set to a value ensuring that the fluctuation of the power dispatch does not exceed the two corresponding limitations of $\gamma_{1\min}$ and $\gamma_{30\min}$ [16]. In this paper, we determine the smoothing time constant based on the curve expressed by the fluctuation in power with respect to the smoothing time constant. The curve is obtained from the given WT specifications and the historical long-term wind power

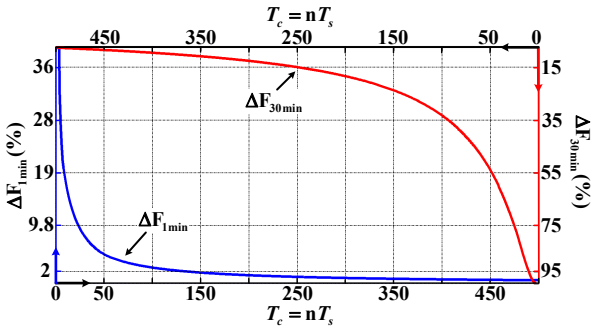

Fig. 9. Fluctuation of power dispatch with respect to the smoothing time constant.

profile. We investigate the proposed smoothing power control based on the ZPLPF defined in (8) with T_c varying from $4T_s$ to $500T_s$. From this, the maximum fluctuations $\Delta F_{1\min}$ and $\Delta F_{30\min}$ of power dispatched in 1 min and 30 min periods are obtained. For example, Fig. 9 shows the curves of $\Delta F_{1\min}$ and $\Delta F_{30\min}$ of a WT with real wind speed data measured on Jeju Island in the year 2012. As expected, both fluctuation indexes $\Delta F_{1\min}$ and $\Delta F_{30\min}$ attenuate exponentially when we increase T_c. If the electric power system requirements for the fluctuation limitations of power dispatched in 1 and 30 min periods are 2% and 15%, respectively, then the smoothing time constant must be higher than $140T_s$ for the first requirement and higher than $250T_s$ for the second. Therefore, we should choose $T_c = 300T_s$ to guarantee that the power dispatch fluctuation is within the acceptable range.

5. Numerical Examples

In order to verify the effectiveness of the proposed dispatching method based on the designed ZPLPF, several simulations are made using MATLAB software. For the assessment, a PMSG-WT with a 3 MW power rating is selected [24] and the real wind speed on Jeju Island in the year 2012 is measured at 1-min intervals. In order to investigate the fluctuation of power dispatched in 1 min periods, ten samples of wind speed per minute are needed. These samples are obtained by linearly interpolating the measured data and adding noise with zero-mean and 0.01 standard deviation in normal distribution. These additional wind speed data mean the system sampling time to be T_s = 6s. In addition, the wind speed is measured at a height of 10 m, whereas the tower of an industrial WT is usually higher than 50 m; hence, the wind speed at the hub of a WT needs to be interpolated. To do this, the Hellman equation is used with the WT hub height equal to 84 m and the Hellman exponential coefficient $\alpha = 0.4$ [25].

In order to reduce the simulation time while still determining the effect of seasonal changes on wind power characteristics, the study is carried out over four separate months to represent the four seasons: March for spring,

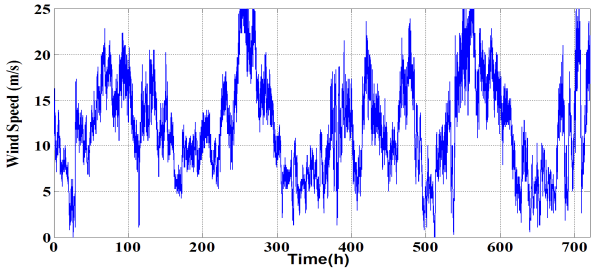

Fig. 10. Wind speed profile from March 2012.

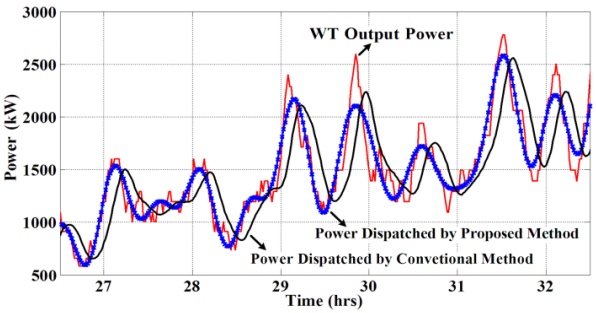

(a)

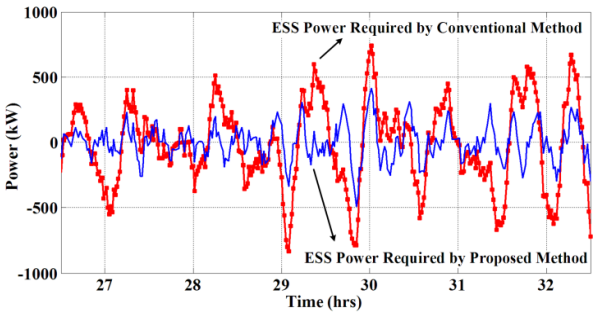

(b)

Fig. 11. (a) WT output power and power delivered to grid; (b) ESS power flow.

June for summer, September for autumn, and December for winter. The performance of the proposed dispatching method using the designed ZPLPF is compared with that of the conventional method adopting the IFLPF. The smoothing time constant of the filter is set with $T_c = 300T_s$ or $T_c = 30$ min based on the relationship shown in Fig. 9.

Fig. 10 shows the wind speed data collected in March. The wind speed is highly variable, which leads to high fluctuations in the WT output power. The ESS is employed to attenuate fluctuations. The power and energy ratings, which are determined by (4)-(6), depend on the dispatching power flow. Fig. 11(a) illustrates the WT output power, the power dispatch by the proposed dispatching method, and the power dispatch by the conventional method. Compared with the conventional dispatching method, the proposed method can eliminate the delay problem; this greatly reduces the ESS power capacity as shown in Fig. 11(b). At any instant, the ESS power required in the conventional method is significantly higher than that of the proposed

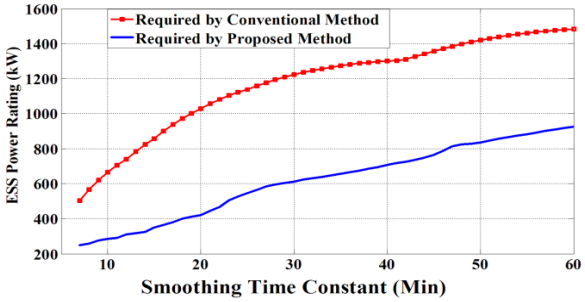

(a)

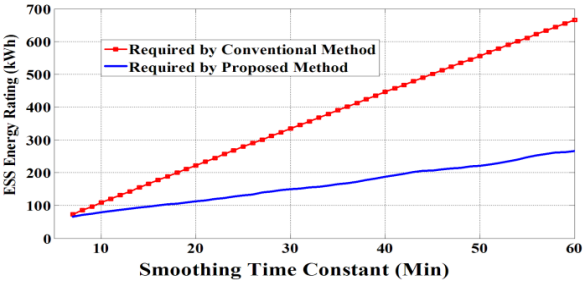

(b)

Fig. 12. Required ESS capacity with respect to the cut-off frequency: (a) Power rating; (b) Energy rating.

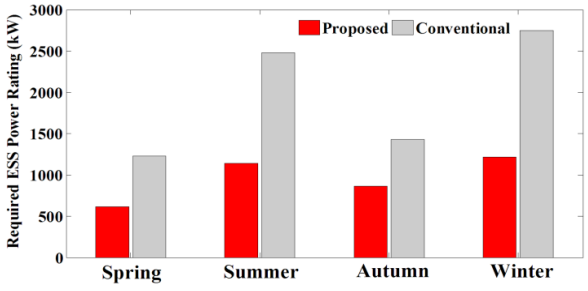

(a)

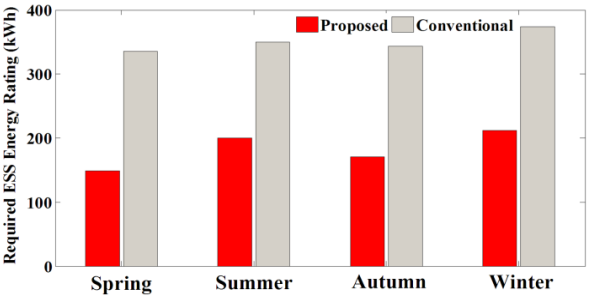

(b)

Fig. 13. Required ESS capacity according to the season: (a) ESS power rating; (b) ESS energy rating.

method. This means that the required ESS capacity in the proposed method is much lower than that of the conventional method; hence, the system cost can be reduced. For greater clarity and detail, the ESS capacity (including energy and power ratings) is calculated and shown in Fig. 12. This data is calculated using the wind speed profile from March and demonstrates the effect of using smoothing time constants varying from $40T_s$ (4 min) to $600T_s$ (60 min). Both the conventional and proposed methods require higher ESS capacity as the smoothing time constant is increased. However, we can see that for any smoothing time constant, the ESS capacity in the proposed dispatching method is significantly reduced. For instance, when the smoothing time constant is 30 min, the ESS capacity with the conventional method is 1225 kW/335 kWh whereas the proposed method requires only 615 kW/150 kWh as shown in Figs. 12(a) and (b) for the power and energy ratings, respectively.

The required ESS capacity with respect to the season is plotted in Fig. 13(a) for power rating and Fig. 13(b) for energy rating. A smoothing time constant of 30 min was used to generate both of these figures. The ESS power rating is significantly impacted by the seasonal weather conditions; the required power rating is highest in the winter. For any season, the proposed method requires lower ESS capacity compared to the conventional method. To ensure that the ESS matches the given attenuation level of the WT output power fluctuation in a year, the ESS capacity is derived from the winter season: 2750 kW/375 kWh for the conventional dispatching method and 1220 kW/215 kWh for the proposed method.

6. Conclusion

In this paper, an optimal dispatching power control method is proposed to overcome response delay. We have determined that the ESS capacity increases when the phase delay of the IFLPF appears in the conventional smoothing power control method. The suggested ZPLPF has no phase delay, and it can be designed with a simple process and a small number of coefficients. Due to the zero phase delay in the proposed smoothing power control, the ESS capacity is reduced significantly compared with that of the conventional method. Therefore, the proposed method represents a feasible and optimal solution for dispatching wind power into the grid. To demonstrate the superiority of the proposed dispatching method, a 3 MW PMSG-WT is studied to dispatch power into the grid using real wind speeds measured on Jeju Island. The results prove that, at any attenuation levels or on any the seasons, the proposed dispatching method achieves a much smaller ESS capacity compared with the conventional method.

Acknowledgement

This work was supported by the National Research Foundation of Korea Grant funded by the Korean Government (2013R1A2A2A01016398).

References

[1] R. Teodorescu, M. Liserre, and P. Rodríguez, "Grid Converters for Photovoltaic and Wind Power Systems," *John Wiley & Sons,* 2011.

[2] S. Teleke,M. E. Baran, S. Bhattacharya, and A. Q. Huang, "Rule-Based Control of Battery Energy Storage for Dispatching Intermittent Renewable Sources," *IEEE Trans. Sustain. Energy,* vol. 1, no. 3, pp. 117-124, Oct. 2010.

[3] Renewables 2012 Global Status Report [Online]: http:// www.map.ren21.net/GSR/GSR2012_low.pdf.

[4] C. Luo and B. T. Ooi, "Frequency Deviation of Thermal Power Plants due to Wind Farms," *IEEE Trans. Energy Convers.,* vol. 21, no. 3, pp. 708-716, Sept. 2006.

[5] J. K. Lyu, M. K. Kim, and J. K. Park, "Impacts of Wind Power Integration on Generation Dispatch in Power Systems," *J. Electr. Eng. Technol.*, vol. 8, no. 3, pp. 238-243, May 2013.

[6] T. Senjyu, R. Sakamoto, N. Urasaki, T. Funabashi, H. Fujita, and H. Sekine, "Output Power Leveling of Wind Turbine Generator for all Operating Regions by Pitch Angle Control," *IEEE Trans. Energy Convers.,* vol. 21, no. 2, pp. 467-475, Jun. 2006.

[7] D. L. Yao, S. S. Choi, K. J. Tseng, T. T. Lie, "Determination of Short-Term Power Dispatch Schedule for a Wind Farm Incorporated with Dual-Battery Energy Storage Scheme," *IEEE Trans. Sustain. Energy,* vol. 3, no. 1, pp. 74-84, Jan. 2012.

[8] X. Y. Wang, D. V. Mahinda, and S. S. Choi, "Determination of Battery Storage Capacity in Energy Buffer for Wind Farm," *IEEE Trans. Energy Convers.,* vol. 23, no. 3, pp. 868-878, Sept. 2008.

[9] S. Teleke, M. E. Baran, S. Bhattacharya, and A. Q. Huang, "Optimal Control of Battery Energy Storage for Wind Farm Dispatching," *IEEE Trans. Energy Convers.,* vol. 25, no. 3, pp. 787-794, Sept. 2010.

[10] K. W. Wee, S. S. Choi, and D. M. Vilathgamuwa, "Design of a Least-Cost Battery-Supercapacitor Energy Storage System for Realizing Dispatchable Wind Power," *IEEE Trans. Sustain. Energy,* vol. 4, no. 3, pp. 786-796, Jul. 2013.

[11] Q. Li, S. S. Choi, Y. Yuan, and D. L. Yao, "On the Determination of Battery Energy Storage Capacity and Short-Term Power Dispatch of a Wind Farm," *IEEE Trans. Sustain. Energy*, vol. 2, no. 2, pp. 148-158, Apr. 2011.

[12] C. L. Nguyen, T. W. Chun, and H. H. Lee, "Determination of the Optimal Battery Capacity Based on a Life Time Cost Function in Wind Farm," *Energy Conversion Congress and Exposition (ECCE), 2013 IEEE*, CO. USA, pp. 51-58, Sept. 2013

[13] K. Yoshimoto, T. Nanahara, and G. Koshimizu, "New Control Method for Regulating State-of-Charge of a Battery in Hybrid Wind Power/Battery Energy Storage System," *IEEE PES Power Systems Conf. and Expo.,* pp. 1244-1251, Oct.29-Nov.1 2006.

[14] C.L. Nguyen, H.J. Kim, T.S. Lee, and H.H. Lee, "An Effective Dispatching Power Control to Minimize Energy Storage System in Wind Farm," *International Smart Grid Conference & Exhibition 2013,* Jeju, Korea, pp. 600-606, Jul. 2013.

[15] Q. Jiang and H. Wang, "Two-Time-Scale Coordination Control for a Battery Energy Storage System to Mitigate Wind Power Fluctuations," *IEEE Trans. Energy Convers.,* vol. 28, no. 1, pp. 52-61, Mar. 2013.

[16] Q. Jiang, Y. Gong, and H. Wang, "A Battery Energy Storage System Dual-Layer Control Strategy for Mitigating Wind Farm Fluctuations," *IEEE Trans. Power Sys.,* vol. 28, no. 3, pp. 3263-3273, Aug. 2013.

[17] M. A. Tankari, M. B. Camara, B. Dakyo, and C. Nichita, "Wind Power Integration in Hybrid Power System Active Energy Management," *2009 Ecol. Vehicle & Renew. Energy Conf.,* pp. 1-6, Mar. 2009.

[18] H. Li, and Z. Chen, "Overview of Different Wind Generator Systems and Their Comparisons," *IET Renew. Power Generation,* vol. 2, no. 2, pp. 123-138, Jun. 2008.

[19] J. N. Baker and A. Collinson, "Electrical Energy Storage at the Turn of the Millennium," *Inst. Elect. Eng. Power Eng. J.,* vol. 13, no. 3, pp. 107-112, Jun. 1999.

[20] P. Pinson and H. Madsen, "Probabilistic Forecasting of Wind Power at the Minute Time-Scale with Markov-Switching Autoregressive Models," *Probabilistic Methods Applied to Power Systems, PMAPS'08*, pp. 1-8, May 2008.

[21] Chi Tsong Chen, "Digital Signal Processing- Spectral Computation and Filter Design," *Oxford Univ. Press,* chap. 7, pp. 294-313, 2001.

[22] H. V. Brussel, C. H. Chen, and J. Swevers, "Accurate Motion Controller Design Based on an Extended Pole Placement Method and a Disturbance Observer," *Ann. CIRP,* vol. 43, no. 1, pp. 367-772, 1994.

[23] C.J. Kempf and S.Kobayashi, "Disturbance Observer and Feed-Forward Design for a High-Speed Disk-Drive Positioning Table," *IEEE Trans. Contr. Sys. Tech.,* vol. 7, no. 5, pp. 513-525, Sept. 1999.

[24] V112-3.0MW [Online]. Available: http://creative-energyalternatives.com/wind/Vestas_V_112_web_100309.pdf.

[25] S. Heier, "Grid Integration of Wind Energy Conversion Systems," *John Wiley & Sons.* pp. 45, 2nd Edition, 2006.

Cong-Long Nguyen was born in Nghe-An province, Vietnam, in 1987. He received the B.S. degree in Electrical Engineering from the University of Technology, Ho Chi Minh City, Vietnam, in 2010. He worked at the Intel Corporation as a production engineer in Vietnam site. Currently, he is a research assistant at the University of Ulsan, Ulsan, Korea to work toward the Ph.D. degree in Electrical Engineering. His research interests include power electronics applied to electric vehicles, power quality control, and optimization of electric energy storages in renewable energy conversion systems.

Hong-Hee Lee is a Professor in the School of Electrical Engineering, University of Ulsan, Ulsan, Korea. He is also the Director of the Network-based Research Center (NARC). He received his B.S., M.S., and Ph.D. in Electrical Engineering from Seoul National University, Seoul, Korea, in 1980, 1982, and 1990, respectively. His current research interests include power electronics, network-based motor control, and renewable energy. He is a senior member of the Institute of Electrical and Electronics Engineers (IEEE), the Korean Institute of Power Electronics (KIPE), the Korean Institute of Electrical Engineers (KIEE), and the Institute of Control, Robotics, and Systems (ICROS).